

SINGLE-PASS SEA/ICE DISCRIMINATION USING ERS-2 SCATTEROMETER DATA

Xavier Neyt, Pauline Pettiaux, Nicolas Manise and Marc Acheroy

Royal Military Academy, Brussels, Belgium

ABSTRACT

This paper presents a new method to perform sea/ice discrimination in single-pass ERS-2 scatterometer data. Existing methods are first reviewed and compared in a consistent framework. Next, the ice probability according to the individual existing methods is learned through the use of a neural network. Finally, the individual criteria are combined together in order to increase the sea-ice discrimination accuracy. The proposed method is shown to provide an acceptable performance even on single-pass data, i.e., without requiring temporal averaging.

Keywords: Scatterometry, ice discrimination, neural network

1. INTRODUCTION

Besides the study of the ice coverage at the poles, discrimination between open sea and ice is relevant to sea-surface wind extraction using scatterometer data since no wind can be extracted over ice-covered areas. Indeed, winds obtained from ERS-2 σ^o triplets, $(\sigma_f^o, \sigma_m^o, \sigma_a^o)$ measured respectively by the fore, mid and aft antenna, are ambiguous and removing this ambiguity requires spatial coherence of the wind field. Hence, having erroneous wind vectors disturbs the wind ambiguity removal process. Moreover, from an operational point of view and taking into account the near real-time dissemination

Further author information: (Send correspondence to Xavier Neyt) E-mail: Xavier.Neyt@rma.ac.be, Telephone: +32 2 737 6473, Address: Signal and Image Center, Electrical Engineering Dept, Royal Military Academy, 30 av de la Renaissance, B-1000 Brussels, Belgium

requirement, it is advantageous to be able to discriminate ice from open-sea using only the data acquired during the pass being processed.

Several criteria for ice discrimination have been proposed in the literature. In Section 2, these different criteria are reviewed. Section 3 compares the performances of each of these criteria in order to assess the conditions under which they are discriminant. This is done using a neural network architecture. The network is trained to “learn” the ice-probability according to the considered training set. After training, the network is able to provide an ice probability based on one single measurement. In the same section, we propose to combine the output of individual criteria to a single result. Finally, the performance of the overall scheme is discussed.

2. REVIEW OF EXISTING SEA/ICE DISCRIMINATION CRITERIA

2.1. Introduction

The basis of the discrimination is that the statistics of the σ^o measurements over sea is different than that of measurements over ice, as illustrated in figure 1. However, the ice and sea scatterers are not

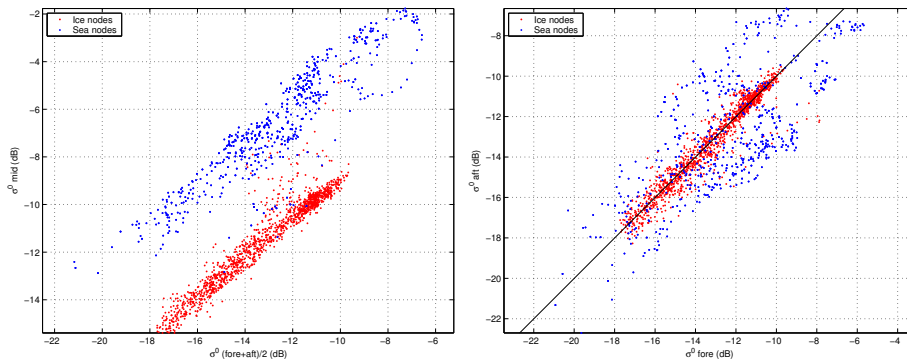


Figure 1. Scatter plot of the σ^o over ice and over sea for node 5 (low incidence angle). Left: projection in the $\sigma_f^o = \sigma_a^o$ plane, Right: projection in the $\sigma_m^o = 0$ plane.

always well separated. In particular, for higher incidence angle, both classes can get very close to each other as figure 2 illustrates.

Besides the raw σ^o -triplet, other classification metrics have been proposed in the literature. These will be reviewed below. The graphs in the following sections are obtained using data corresponding

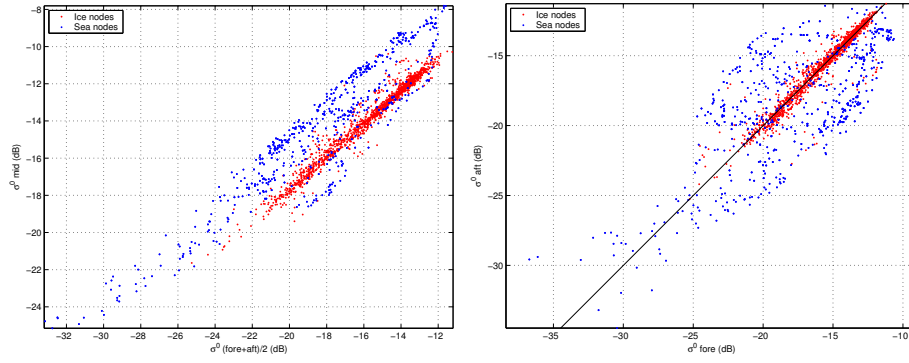


Figure 2. Scatter plot of the σ^o over ice and over sea for node 15 (high incidence angle). Left: projection in the $\sigma_f = \sigma_a$ plane, Right: projection in the $\sigma_m^o = 0$ plane.

to two passes over the North pole on December 30th 1999.

2.2. Isotropy

$I_n^{1,2}$ a measure of the isotropy of the backscattering is proposed as discriminating criterion. The isotropy factor is defined as

$$\mathcal{A} = \left| \frac{\sigma_f - \sigma_a}{\sigma_f + \sigma_a} \right| \quad (1)$$

where the σ are provided in dB.

Open sea typically results in a high isotropy factor, while sea-ice corresponds to rather low isotropy factor values. However, when the wind is blowing parallel or perpendicular to the ground track, a low isotropy value will be observed over sea. Indeed, in this case, the capillary waves generated by the wind are propagating perpendicular or parallel to the satellite ground track hence the fore and aft measurements will have similar values.

Figure 3 (left) illustrates the repartition of isotropy factor between sea and ice for the various incidence angles. Clearly, the isotropy factor corresponding to sea-ice is typically small. However, as can be seen, small isotropy factor over open sea are possible too.

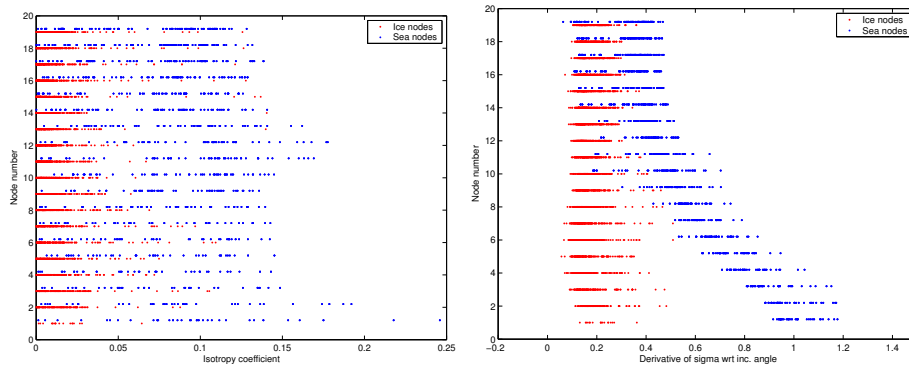


Figure 3. Scatter plot of the isotropy factor (left) and of the derivative of sigma (right), illustrating the distribution of the sea and ice nodes.

2.3. Derivative of backscatter in function of the incidence angle

In,³ the derivative of the σ^o w.r.t. the incidence angle was proposed as discriminating criterion. The derivative is approximated by

$$\mathcal{D} = -\frac{(\sigma_f + \sigma_a)/2 - \sigma_m}{(\theta_f + \theta_a)/2 - \theta_m} \quad (2)$$

where the σ^o values are in dB and the incidence angle values in degrees. Notice that, due to the use of the zero-gyro mode following the gyroscopes anomaly, the incidence angles of the fore and of the aft beam cannot be assumed equal anymore⁴ hence the modification of the original formula given in.³ Measurements over ice typically result in a lower \mathcal{D} than measurements over sea, at least when the incidence angle is not too high.

From figure 3 (right) illustrating the repartition of the derivative between sea and ice nodes for the various incidence angles, it is clear that the criterion is more discriminant for low incidence angles (low node number, near swath).

2.4. Distance to wind model

The (Euclidean) distance to the wind model was also proposed⁵ as a criterion. The reasoning behind this criterion is that measurements acquired over sea should lie close to the wind model, while measurements performed over ice might be located further away from the wind model.

Figure 4 (left) shows that this criterion is hardly discriminating for medium incidence angle. This is related to the fact that for medium incidence angles, σ^0 measurements over ice are actually very close to the wind model.

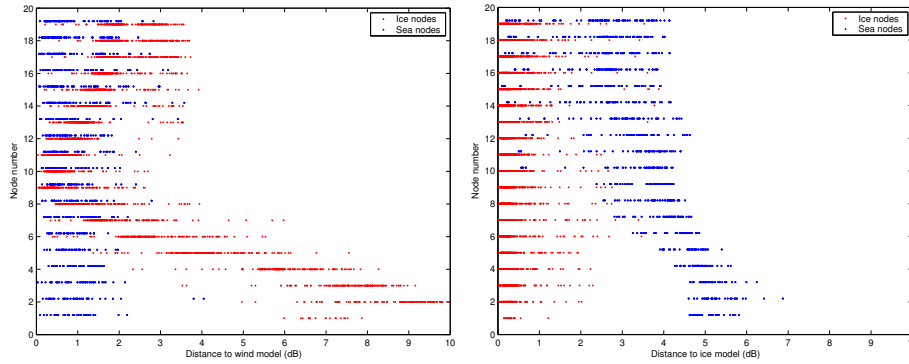


Figure 4. Scatter plot of the distance to the wind model (left) and distance to ice model (right), illustrating the distribution of the sea and ice nodes.

2.5. Distance to ice model

Several models of the σ^0 over ice were proposed.^{6,7} The idea is to use the euclidean distance to the ice-model as discriminating factor. The models selected in this document is the ERS ice model described in.⁷ This model can however be generalized to other types of scatterometers. The model consists in an incidence angle-dependent line. For the details of the computation, the reader is referred to.⁷

As can be seen in figure 4 (right), this metric is essentially discriminant for low incidence angles. Indeed, for higher incidence angles, the distribution of ice and sea nodes tends to be closer to each other as can be seen in figures 1 and 2.

3. SEA ICE DISCRIMINATION

3.1. Introduction

Typically, the criteria described in the previous section are thresholded to determine whether the measurement made corresponds to open sea or to ice.^{1,7} That threshold is also typically dependent on

the incidence angle. However, a binary threshold does not take into account the fact that, in ambiguous cases, it is not possible to make a decision based only on one single σ^0 -triplet measurement. In,⁷ a decision algorithm using 4 classes (sea, ice, mixed and not valid) is proposed. This algorithm is based on an incidence-angle dependent thresholding of the distances to the ice model and to the wind model. The existence of the mixed class acknowledges the fact that some nodes cannot clearly be classified as ice or sea.

These decision methods provide a binary (quaternary) answer regarding the status of the considered measurement point (sea or ice). No information is provided on the (un)certainty of the classification and the classification accuracy trade off is difficult to master. In the following section, we define an ice probability based on the criteria defined in the previous section. This ice probability can then be thresholded to perform a classification. Furthermore, the criteria presented above can be combined together, as individual experts, to provide a combined ice probability.

3.2. A neural-network based classification

Our goal is thus to compute the ice probability given the measurements, $P(H_1|m_{c,i},n_i)$, where H_1 is the hypothesis “the measurement i corresponds to ice”, $m_{c,i}$ is the numerical value of the criterion c for measurement i and n_i is the across-track node number at which measurement i was made.

It is well known⁸ that this probability can be learned by a Multi-Layer Perceptron (MLP). The learning process consists in feeding the MLP with the measurements made $(m_{c,i},n_i)$ and imposing as desired output 1 if H_1 is true for measurement i and 0 else. In order to avoid biasing the MLP output due to a differing a priori probability we must ensure $P(H_1) = P(\overline{H_1})$ over the training set. This imply that the number of measurements corresponding to ice in the training sets must be equal to the number of measurements corresponding to sea.

We considered an MLP with two inputs, one for the value of the criterion $m_{c,i}$ and the other for the node number n_i . It has one single hidden layer counting 5 neurons. The number of hidden layers and the number of neurones in these layers govern the complexity of the non-linear function that the MLP will be able to approximate. We are actually seeking to approximate reasonably “simple” functions, hence the single hidden layer and the small number of neurons in that hidden layer.

The results of the learning of the probability by the MLP for the different criteria are shown in figure 5. For clarity, the 3D-surface was thresholded. As can be seen from this figure, the uncertain areas for the sigma anisotropy and for the distance to wind model criteria are quite large. In itself a large uncertain area is not bad, as long as no measurement samples fall inside that area. As can be seen by comparing figure 5 with the figures from Section 2, there are actually a lot of samples that fall inside that uncertain area for the Isotropy and for the Distance to the wind model criteria. Consequently, these methods exhibit a high rate of “No Decision” answers.

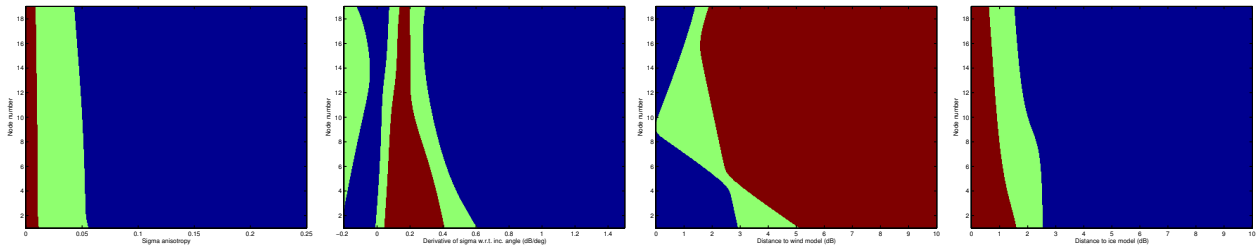


Figure 5. Thresholded probability $P(H_1|m_{c,i},n_i)$ for each of the criteria described in Section 2, where blue corresponds to $P < 20\%$ (open sea with 80% probability), red to $P > 80\%$ (ice with 80% probability) and green to values in between (mixed or unknown).

3.3. Performance comparison

The output of the MLP provides the probability that a given input corresponds to ice (H_1). By thresholding the output probability, a decision can be taken regarding the class to which the provided input belong. For a given threshold, it is possible to compute the True Ice rate (measurements classified as ice and actually corresponding to ice), False Sea rate (measurements classified as ice, but actually corresponding to sea) and unclassified ice (measurement not classified although it was actually ice). Figure 6 (left) shows the ROC for ice, where the independent variable is the threshold used in taking the decision. As can be seen, the “Distance to ice model” criterion is the most discriminant, closely followed by the “Derivative of sigma”. The two other criteria would imply a much lower True Ice rate if a low False sea rate was to be achieved. Figure 6 (right) shows the unclassified ice rate in function of the across track node-number (which corresponds approximatively to an incidence angle). As can be seen, the “Distance to wind model” criterion fails to discriminate between ice and sea at

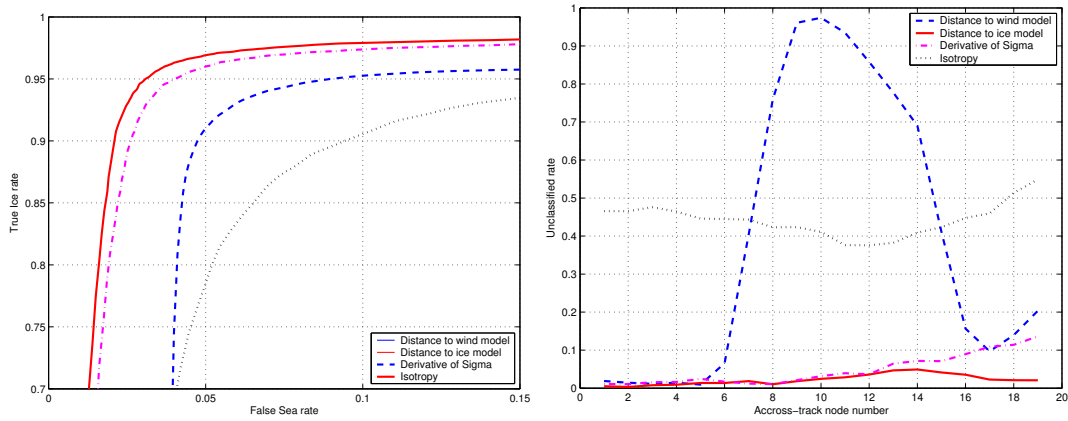


Figure 6. Comparison between the different criteria: ROC curve for the 4 criteria (left) and “No Decision” rate for a False Ice rate of 3% (right).

mid swath. This is due to the fact that at those incidence angles, σ^o corresponding to ice are also very close to the wind model. Also, the σ^o “Isotropy” criterion does not prove to be very decisive at any incidence angle. This confirms the deductions made in Section 2.

3.4. Fusion

When several sources of information are available, they can be combined to reduce imprecision and uncertainty and increase completeness.⁹ A good review of some of the existing combination methods is to be found in.⁹ It only makes sense to combine the “best” sources of information, hence we will combine the “Distance to ice model” and the “Derivative of sigma” criteria. . We will compare two combination methods: the mean operator and the symmetrical associative sums. The mean operator simply outputs the mean of its inputs, i.e. $s(x,y) = (x + y)/2$, where $x,y \in [0, 1]$ are the two inputs probabilities to be combined and $s(x,y)$ is the resulting output. It is obvious that this operator always makes a compromise between its inputs. The symmetrical associative sum that we considered is given by $s(x,y) = \frac{xy}{1-x-y+2xy}$ (same definition for x, y and s as above). This operator has a behavior that depends on the input data. It will tend to a compromise if the inputs do not agree. On the other hand, if the inputs do agree, it will reinforce the agreement. Figure 7 (left) compares the performance of the two selected criteria (“Distance to ice model” and “Derivative of sigma”) with those obtained after combination of these two criteria using each of the two selected fusion operators. The ROC

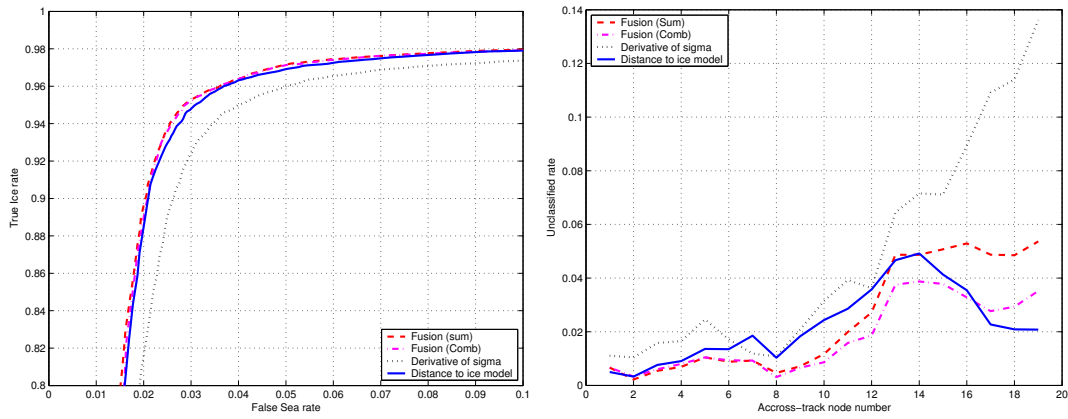


Figure 7. Comparison of the performance of the fusion: ROC curve (left) and “No Decision” rate for a False Ice rate of 3% (right).

curves of the combinations are slightly above that of the best single criterion, which means that the True Ice rate will be higher for the same False Sea rate. Figure 7 (right) compare the “No Decision” rate of the same decision methods in function of the across-track node number. The combination has the effect of reducing the “No Decision” rate but for large node numbers. This is particularly true for the Symmetrical associative sum operator. The lower performance at large node numbers is due to the fact that the performance of the “Derivative of sigma” criterion has a lower decisiveness for large node numbers. Table 1 shows the performance figures for the two individual criteria and the proposed combination methods.

| | Deriv. of σ | Dist. to ice model | Mean | Sym. As. Sum |
|------------------|--------------------|--------------------|--------|--------------|
| True Ice rate | 92.23% | 94.73% | 95.21% | 95.23% |
| Unknown Ice rate | 4.81% | 2.28% | 1.82% | 1.78% |

Table 1. Performance comparison at a False Sea rate of 3%.

4. CONCLUSIONS

In this paper, we presented a Neural-Network based method to compare the various ice detection criteria found in the literature. We also showed that by combining the two best criteria, a yet better

performance was achieved. This performance was obtained in a scenario where single observations are considered, i.e., excluding any kind of time-averaging.

ACKNOWLEDGMENTS

This work was performed under European Space Agency (ESA) contracts. We would like to thank the ESA for the use of data and the provision of industry-confidential information. This work would not have been possible without the help of Pascal Lecomte and Raffaele Crapolichio from the European Space Agency/ESRIN.

REFERENCES

1. P. Lecomte, "Wind scatterometer processing requirements for ice detection," Tech. Rep. ER-SA-ESA-SY-1122, ESA ESRIN, Sept. 1993. ERS-2 A8.
2. A. Cavanié, F. Gohin, Y. Quilfen, and P. Lecomte, "Identification of sea ice zones using the AMI-wind: Physical bases and applications to the FDP and CERSAT processing chains," in *Proc. Second ERS-1 Validation Workshop*, pp. 1009–1012, ESTEC, (Hamburg, Germany), Oct. 1993.
3. F. Gohin and A. Cavanié, "Some active and passive microwave signatures of antarctic sea ice from mid-winter to spring 1991," *International Journal of Remote Sensing* **16**(11), pp. 2031–2054, 1995.
4. X. Neyt, P. Pettiaux, and M. Acheroy, "Scatterometer ground processing review for gyro-less operations," in *Proceedings of SPIE: Remote Sensing of the Ocean and Sea Ice 2002*, **4880**, 2002.
5. F. Gohin and C. Maroni, "ERS scatterometer polar sea ice grids: User manual," Tech. Rep. C2-MUT-W-03-IF, IFREMER, Mar. 1998.
6. A. Cavanié, "An empirical C-band backscatter model over arctic sea ice from ERS-1 AMI-wind data," in *Proc. of a Joint ESA-Eumetsat Workshop on Emerging Scatterometer Applications*, pp. 99–106, ESTEC, ESTEC, (Noordwijk, The Netherlands), Nov. 1995.
7. S. de Haan and A. Stoffelen, "Ice discrimination using ERS scatterometer," tech. rep., KNMI, Sept. 2001.
8. C. Bishop, *Neural Networks for Pattern Recognition*, Carendon Press, 1995.
9. I. Bloch, "Information combination operators for data fusion: A comparative review with classification," *IEEE Transactions on Systems, Man and Cybernetics* **26**, pp. 52–67, Jan. 1996.